Journal of the Korean Magnetic Resonance Society **2020**, *24*, 136-142
DOI http://dx.doi.org/10.6564/JKMRS.2020.24.4.136

The Structural Studies of Biomimetic Peptides P99 Derived from Apo B-100 by NMR

Gil-Hoon Kim, Ho-Shik Won*

Department of Chemistry and Molecular Engineering, Hanyang University, Ansan 15588, Republic of Korea

Received Dec 10, 2020; Revised Dec 17, 2020; Accepted Dec 18, 2020

Abstract Apolipoprotein B-100 (apo B-100), the main protein component that makes up LDL (Low density lipoprotein), consists of 4,536 amino acids and serves to combine with the LDL receptor. The oxidized LDL peptides by malondialdehyde (MDA) or acetylation in vivo were act as immunoglobulin (Ig) antigens and peptide groups were classified into 7 peptide groups with subsequent 20 amino acids (P1-P302). The biomimetic peptide P99 (KGTYG LSCQR DPNTG RLNGE) out of B-group peptides carrying the highest value of IgM antigens were selected for structural studies that may provide antigen specificity. Circular Dichroism (CD) spectra were measured for peptide secondary structure in the range of 190-260 nm. Experimental results show that P99 has pseudo α-helice and random coil structure. Homonuclear (COSY, TOCSY, NOESY) 2D-NMR experiments were carried out for NMR signal assignments and structure determination for P99. On the basis of these completely assigned NMR spectra and proton distance information, distance geometry (DG) and molecular dynamic (MD) were carried out to determine the structures of P99. The proposed structure was selected by comparisons between experimental NOE spectra and back-calculated 2D NOE results from determined structure showing acceptable agreement. The total Root-Mean-Square-Deviation (RMSD) value of P99 obtained upon superposition of all atoms were in the set range. The solution state P99 has mixed structure of pseudo α-helix and β-turn(Gln[9] to Thr[13]). These NMR results are well consistent with secondary structure from experimental results of circular dichroism. Structural studies based on NMR may contribute to the prevent oxidation studies of atherosclerosis and observed conformational characteristics of apo B-100 in LDL using monoclonal antibodies.

Keywords Apolipoprotein B-100, Immunoglobulin, Molecular dynamic computation, NMR

Introduction

Apolipoproteins playing an important role in lipid transport and metabolic process in blood stream are components of LDL and HDL. Apolipoproteins are classified into A-I, A-II, B, C-I, C-II, D, E, respectively, based on the ABC nomenclature. There are three main lipoprotein classes according to density: very low density lipoproteins (VLDL), low density lipoproteins (LDL, d:1.019-1.063 g/mL), and high density lipoproteins (HDL, d:1.063-1.21 g/mL).[1] Studies relating to the structure and metabolism of LDL are important because of the direct correlation between atherosclerosis and high LDL levels in human plasma. LDL is the end product of VLDL catabolism and the major cholesterol transporting

* Address correspondence to: **Ho-Shik Won,** Department of Chemical and Mole Engineering, Hanyang University, 5 5,Hanyang Deahak-Ro, Sangrok-Gu, Ansan, 15588, Republic of Korea, Tel: 031-400-5497, E-mail: hswon@hanyang.ac.kr

lipoprotein in human plasma. The majority of LDL particles contain a single apolipoprotein called apo B-100.[1,2] After the elucidation of the role of apolipoproteins in the regulation of lipoprotein metabolism, it became apparent that improvements in the characterization of apo B-100 were needed to facilitate the development of the linkage between LDL and atherosclerosis.[1]

Apolipoprotein B is the largest and one of the most important proteins that cover the lipid surfaces of lipoproteins. Apo B exists in two forms, apo B-100 and apo B-48.[3] Apolipoprotein B (apo B) is the major protein component of plasma LDL. It plays functional roles in lipoprotein bio-synthesis in liver and intestine, and is the ligand recognized by the LDL receptor during receptor mediated endocytosis.[4] Apo B-100 which consists of 4,536 amino acids has a molecular mass of 513 kDa and its levels of both LDL-cholesterol and plasma apo B are correlated with coronary heart.[5] The structure of human apo B has been analyzed in term of its functions in lipid binding, lipoprotein assembly and as the ligand responsible for LDL clearance by the LDL receptor pathway.[6-8] In apo B-100 few of the predicted α-helices are truly amphipathic in terms of charge distribution on the polar surface except for one extended region which contains good examples of amphipathic α-helices, and may contribute to lipid binding. The secondary structure of apo B-100 has been suggested to consist of 43% α-helical, 21% β-sheet, 16% β-turn and 20% random structure.[9-10] The β-structure of apo B-100 is thought to be responsible for its interaction with lipids, due to its high hydrophobicity, but is not confined to a particular region and various sections of the protein are buried in the lipid moiety.[11]

Recently, computer modeling studies based upon biochemical analyses have shown that large segment of the apo B backbone have a high amphipathic structure predicted to bind lipid. If these amphipathic β-sheets and α-helices are not folded and associated with lipid in the proper temporal sequence, the structural model predicts that the hydrophobic surfaces would become unstable in the aqueous environment of the endoplasmic reticulum (ER) lumen, leading to improper folding of nascent apo B and eventual degradation.[12,13]

Apo B-100 has 357 lysine residues per molecules, because this protein is intimately associated with lipid in the LDL particles.[14] These lysine residues has highly conjugate with MDA (malondialdehyde) during lipid peroxidation. During the peroxidative modification of LDL products to apo B occurs primarily covalent linkage to epsilon amino groups of lysine residues. If oxidized LDL contains lysine residues conjugated to a number of such fatty acid fragments, the occurrence of oxidatively modified LDL in vivo could be demonstrated by its recognition by mono specific antibodies directed against the various lysine adducts.[6,15]

Conformational studies for biomimetic peptide P99 (KGTYG LSCQR DPNTG RLNGE) recognized by the monoclonal antibodies will be discussed from computer simulation analysis in this study.[16,17]

2D-NMR (COSY, TOCSY, NOESY) experiments were performed using peptide. Circular Dichroism (CD) spectra were compared for peptide secondary structure.[18] Electronic circular dichroism (CD) is the most extensively used spectroscopic technique to determine global secondary structural information in peptides and proteins in solution. NMR signal assignments were accomplished by using 2D-NMR experiments. On the basis of these distance data from NOESY experiments, Distance Geometry (DG) and Molecular Dynamics(MD) were carried out to obtain the tertiary structure of biomimetic peptide P99.[16-19]

Experimental Methods

Sample preparation- Apo B-100 biomimetic peptide P99 (KGTYG LSCQR DPNTG RLNGE) was obtained from Peptron Inc. Peptide was synthesized using solid-phase method. The water soluble P99 was dissolved at 3.46 mM concentration in 400 μL DMSO-d_6 for NMR experiments and 0.46 μM in D_2O for Circular dichroism measurement.[19]

NMR experiments- All NMR experiments were performed by using the 500 MHz (499.94 MHz) Varian spectrometer at 298 K. 2D NMR experiments

included COSY, TOCSY, NOESY were performed with a 512×2048 data matrix size with 32 scans per t1 increment and spectra were zero filled of 2048×2048 data points. TOCSY spectrum was collected with a mixing time of 80 ms, MLEV-17 spin lock pulse sequence. Although NOESY experiments were recorded at two different 300 ms and 400 ms mixing time, the NOE spectrum at 300 ms mixing time was used for signal assignment and 2D NOE back-calculation. Data were processed and analyzed on a SGI Octane workstation using Felix and NMR ViewJ software (9.2.b20). NMRViewJ was also used for sequential assignment of each amino acid.[16,19]

CD measurements- Secondary structure of P99 was obtained using the Chiralscan-plus spectrophotometer at 298K. Measurements at 190-260 nm were made in a 1.0 cm quartz cell. CD measurements are reported as mean residue ellipticity at a given wavelength of peptide and sample data were processed using the CDNN (ver2.1).[18]

Solution state structure determination- Biomimetic peptide structure determinations were carried out using HYGEOM™ and HYNMR™. Sequential assignments of amino acid spin systems were made using TOCSY and NOESY spectra. Most important, direct way for secondary structure determination based on qualitative analysis of NOE. The structures were calculated from the NMR data according to the standard HYGEOM™ simulated annealing and refinement protocols with minor modifications. Most of distance geometry (DG) algorithm accepts the input of proton-proton distance constraints from NOE measurements. The structure was calculated using the DG algorithm HYGEOM™, and separated structures were generated using all of the constraints and random input. No further refinement by energy minimization was carried out on the output of the DG calculations. Root mean square distances (RMSD) deviations between the NMR structures were 0.33 Å for the backbone. Back calculation was assigned to HYNOE calculation in order to generate the theoretical NOEs. A consecutive serial files, obtained from HYNOE calculation, were incorporated into HYNMR™ to generate NOE back calculation spectra which can be directly compared with experimental NOESY spectra.[16,19]

Results and Discussion

NMR signal assignment- Connectivities derived from through bond J-coupling and through space coupling are important in NMR signal assignment and solution state structure determination. The proton-proton connectivities that identify the different amino acid type are established via scalar spin-spin coupling, using COSY and TOCSY.

Complete NMR signal assignments listed in Table 1 were accomplished by using homonuclear COSY and TOCSY experiments. Assignments using sequential NOEs can be obtained for proteins with natural isotope distribution. Relations between protons in sequentially neighboring amino acid residues i and i+1 are established by NOEs manifesting close approach among $d_{\alpha N}$, d_{NN}, $d_{\beta N}$. Except for flexible terminal amino acid residue Pro[12]. The correlating signals of adjacent residues on the basis of dipolar connectivities obtained from 2D NOE spectra are listed in Table 2. Dipolar connectivities from amide protons to α- and amide protons were also used for sequential signal assignments, and the fingerprint region of the NOE spectra recorded at 300 ms are shown in Figure 1. Structure calculation was used to many inter and intra residue NOE connectivities. Table 2 indicates the important NOE connectivities used for the peptide structure determination. Specific conformation of peptide P99 are observed to be $Gly[2]_{\alpha H}$ - $Thr[3]_{NH}$, $Tyr[4]_{\alpha H}$ - $Asp[11]_{NH}$, $Pro[12]_{\alpha H}$ - $Gly[19]_{NH}$ Although relatively weak $d_{\alpha N}$ (i, i+2) dipolar connectivities from $Gly[2]_{\alpha H}$ - $Tyr[4]_{NH}$, $Thr[14]_{\alpha H}$ - $Arg[16]_{NH}$ were observed, it was apparent that the P99 has a characteristic conformation including a α-helice form and partial β-turn. In order to determine the DG structure, several variable velocities simulated annealing and conjugate gradient minimization steps were used in the refinement scheme. Addition of restraints to account for minor differences between experimental and back calculate spectra enabled the generation of new DG structures with substantially reduced penalties. To determine which of the DG structures most accurately reflect

the experimental NOESY data, 2D NOESY back calculations were carried out. As illustrated in Figure 3, back calculated spectrum of the P1 was generally consistent with the experimental NOESY data and best positioned DG structure are shown in Figure 5.

Table 1. ^{1}H-NMR chemical shifts of P99

Residue	NH	αH	βH	γH	Others
Lys[1]	8.344	4.024	1.920	1.575	δH : 1.738 εH : 2.965
Gly[2]	8.879	4.025 4.153	-	-	-
Thr[3]	8.156	4.476	4.166	1.203	-
Tyr[4]	8.140	4.662	2.927 3.133	-	δH : 7.237 εH : 6.832
Gly[5]	8.444	3.941	-	-	-
Leu[6]	8.161	4.636	1.678	1.800	δCH_3 : 1.067 1.095
Ser[7]	8.374	4.524	3.818	-	-
Cys[8]	8.237	4.632	2.599 2.982	-	-
Gln[9]	8.276	4.443	1.941	2.077 2.312	εNH : 7.031 7.458
Arg[10]	8.201	4.468	1.845	1.677	δH : 3.283 εNH : 7.690
Asp[11]	8.556	4.979	2.665 2.969	-	-
Pro[12]		4.521	2.223	2.064	δH : 3.820
Asn[13]	8.279	4.787	2.643 2.822	-	δNH_2 : 7.219 7.650
Thr[14]	7.777	4.322	4.261	1.258	-
Gly[15]	8.345	3.947	-	-	-
Arg[16]	8.084	4.529	1.889	1.682	εNH : 7.671
Leu[17]	8.231	4.508	1.681	1.807	δCH_3 : 1.048 1.090
Asn[18]	8.281	4.686	2.702 2.751	-	δNH_2 : 7.160 7.658
Gly[19]	8.239	3.836 3.983	-	-	-
Glu[20]	8.239	4.428	2.020 2.188	2.479	-

Table 2. Important NOE connectivities used for the structure determination of P99

Residue	δ(ppm)	NOE connectivities
Gly[2]$_{NH}$	8.879	$G^{2}{}_{\alpha H}$(v.w), $T^{3}{}_{NH}$(v.w)
Gly[2]$_{\alpha H}$	4.153	$T^{3}{}_{NH}$(s), $Y^{4}{}_{NH}$(v.w)
Tyr[4]$_{NH}$	8.140	$Y^{4}{}_{\alpha H}$(w), $Y^{4}{}_{\varepsilon H}$(v.w), $G^{5}{}_{NH}$(w)
Tyr[4]$_{\alpha H}$	4.662	$Y^{4}{}_{\beta H}$(m), $Y^{4}{}_{\delta H}$(v.w), $G^{5}{}_{NH}$(s)
Gly[5]$_{NH}$	8.444	$G^{5}{}_{\alpha H}$(s), $L^{6}{}_{NH}$(w)
Gly[5]$_{\alpha H}$	3.941	$L^{6}{}_{NH}$(s)
Leu[6]$_{\alpha H}$	4.636	$L^{6}{}_{\beta H}$(w), $L^{6}{}_{\delta H}$(w), $S^{7}{}_{NH}$(s)
Leu[6]$_{\beta H}$	1.678	$L^{6}{}_{\gamma H}$(s), $L^{6}{}_{\delta H}$(m), $S^{7}{}_{NH}$(v.w)
Ser[7]$_{NH}$	8.374	$S^{7}{}_{\alpha H}$(w), $S^{7}{}_{\beta H}$(w), $C^{8}{}_{NH}$(w)
Ser[7]$_{\alpha H}$	4.524	$S^{7}{}_{\beta H}$(m), $C^{8}{}_{NH}$(s)
Cys[8]$_{\alpha H}$	4.632	$C^{8}{}_{\beta H}$(w), $Q^{9}{}_{NH}$(s)
Gln[9]$_{\alpha H}$	4.443	$C^{9}{}_{\beta H}$(v.w), $Q^{9}{}_{\gamma H}$(v.w), $R^{10}{}_{NH}$(s)
Gln[9]$_{\beta H}$	1.941	$Q^{9}{}_{\gamma H}$(w), $R^{10}{}_{NH}$(v.w)
Arg[10]$_{NH}$	8.201	$R^{10}{}_{\beta H}$(v.w), $D^{11}{}_{NH}$(v.w)
Arg[10]$_{\alpha H}$	4.468	$R^{10}{}_{\beta H}$(w), $R^{10}{}_{\delta H}$(v.w), $D^{11}{}_{NH}$(v.w)
Arg[10]$_{\beta H}$	1.845	$R^{10}{}_{\gamma H}$(m), $R^{10}{}_{\delta H}$(v.w), $D^{11}{}_{NH}$(v.w)
Asp[11]$_{\alpha H}$	4.979	$D^{11}{}_{\beta H}$(v.w), $P^{12}{}_{\alpha H}$(v.w)
Asp[11]$_{\beta H}$	2.969	$P^{12}{}_{\alpha H}$(v.w)
Pro[12]$_{\alpha H}$	4.521	$P^{12}{}_{\beta H}$(m), $P^{12}{}_{\gamma H}$(w), $P^{12}{}_{\delta H}$(m), $N^{13}{}_{NH}$(v.w)
Pro[12]$_{\beta H}$	2.223	$P^{12}{}_{\gamma H}$(s), $P^{12}{}_{\delta H}$(m), $N^{13}{}_{NH}$(v.w)
Asn[13]$_{NH}$	8.279	$N^{13}{}_{\alpha H}$(w), $T^{14}{}_{NH}$(w)
Asn[13]$_{\alpha H}$	4.787	$N^{13}{}_{\beta H}$(m), $T^{14}{}_{NH}$(s), $G^{15}{}_{NH}$(v.w)
Asn[13]$_{\beta H}$	2.822	$G^{15}{}_{NH}$(v.w)
Thr[14]$_{NH}$	7.777	$T^{14}{}_{\alpha H}$(w), $T^{14}{}_{\beta H}$(v.w), $T^{14}{}_{\gamma H}$(w), $G^{15}{}_{NH}$(w)
Thr[14]$_{\alpha H}$	4.322	$T^{14}{}_{\beta H}$(s), $T^{14}{}_{\gamma H}$(m), $G^{15}{}_{NH}$(m), $R^{16}{}_{NH}$(w)
Thr[14]$_{\beta H}$	4.261	$T^{14}{}_{\gamma H}$(s), $G^{15}{}_{NH}$(v.w), $R^{16}{}_{NH}$(v.w)
Gly[15]$_{NH}$	8.345	$G^{15}{}_{\alpha H}$(s), $R^{16}{}_{NH}$(w)
Gly[15]$_{\alpha H}$	3.947	$R^{16}{}_{NH}$(s), $R^{16}{}_{\alpha H}$(v.w)
Arg[16]$_{NH}$	8.084	$R^{16}{}_{\alpha H}$(w), $R^{16}{}_{\beta H}$(v.w), $L^{17}{}_{NH}$(v.w)
Arg[16]$_{\alpha H}$	4.529	$L^{17}{}_{NH}$(s)
Arg[16]$_{\beta H}$	1.889	$R^{16}{}_{\varepsilon H}$(w), $R^{16}{}_{\delta H}$(vw), $L^{17}{}_{NH}$(v.w)
Leu[17]$_{NH}$	8.231	$L^{17}{}_{\alpha H}$(s), $L^{17}{}_{\beta H}$(s), $L^{17}{}_{\gamma H}$(v.w), $L^{17}{}_{\delta H}$(v.w)
Leu[17]$_{\alpha H}$	4.508	$L^{17}{}_{\beta H}$(s), $L^{17}{}_{\gamma H}$(v.w), $L^{17}{}_{\delta H}$(v.w), $N^{18}{}_{NH}$(s)
Asp[18]$_{\alpha H}$	4.686	$N^{18}{}_{\beta H}$(w), $G^{19}{}_{NH}$(s)
Gly[19]$_{NH}$	8.239	$G^{19}{}_{\alpha H}$(m)

$Glu[20]_{\alpha H}$	4.428	$E^{20}{}_{\beta H}$(v.w), $E^{20}{}_{\gamma H}$(v.w)
$Glu[20]_{\beta H}$	2.188	$E^{20}{}_{\gamma H}$(v.w)

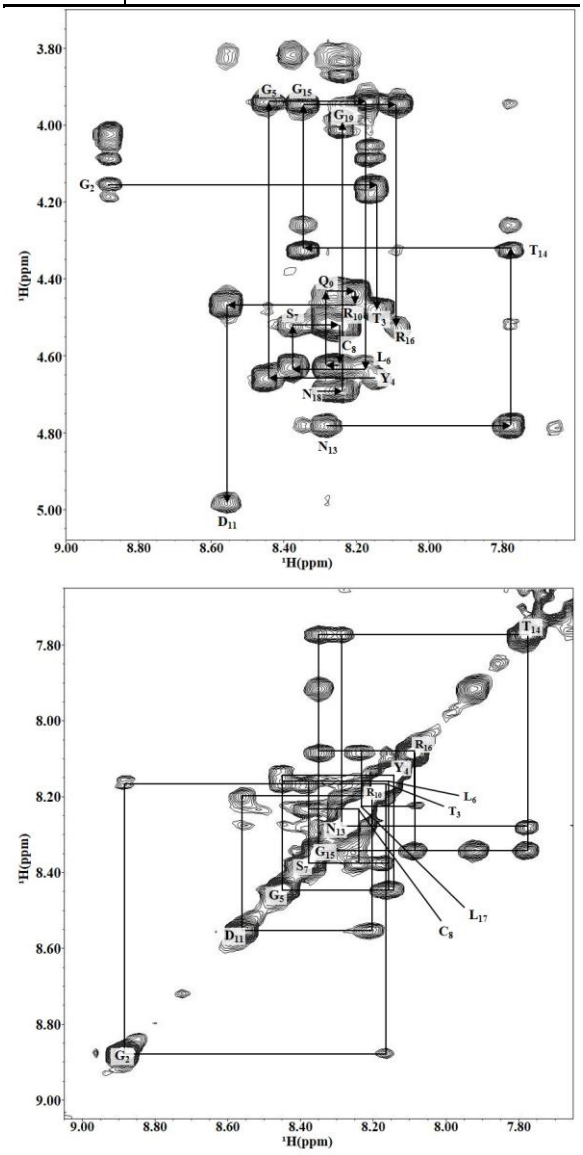

Figure 1. Intraresidue cross peaks labeled in the NH-$C_{\alpha H}$ region (upper), NH-NH region (lower) of the NOE spectra of P99 (τ_m = 300 ms).

Figure 2. NOESY connectivities involving backbone protons for amino acids i and j. The height of the bars symbolizes the relative strength (strong, medium, weak) of the cross peaks in a qualitative way.

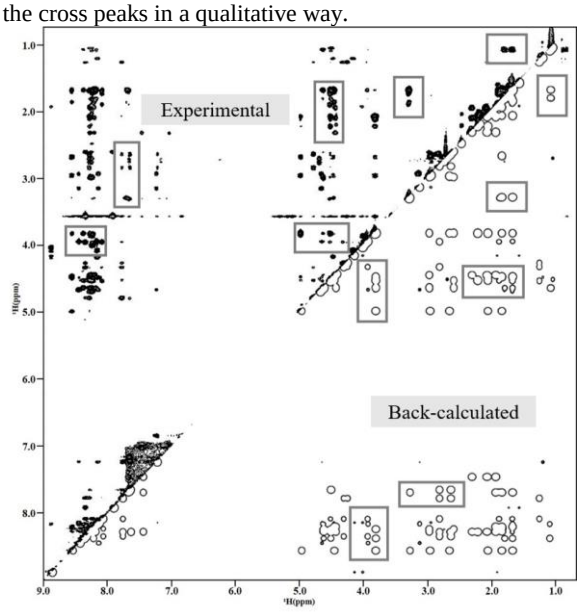

Figure 3. Overlapped comparison of experimental and back-calculation NOESY spectrum of P99 collected at 300 ms mixing time. Each marked site in the figure indicate the similarity between the experiment and the back-calculated of P99 peptide structure

The secondary structure of P99 was analyzed by CD spectrum as shown in figure 4. Peptide carrying an unique conformational motif shows characteristic CD spectrum.

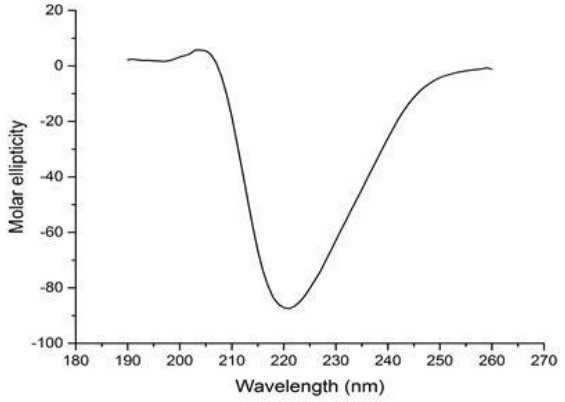

Figure 4. Circular Dichroism spectrum of P99 from 190 to 260 nm at 1.0 nm intervals

The CD spectrum of a protein is basically the sum of

the spectra of its conformational elements, and thus can be used to estimate secondary structure.[18] The result of calculated spectra using the CDNN software shows that P99 peptide contains conformational ratios like 70.2% of α-helices, 6.5% of β-turn, and 19.8% of random coil. The analyzed CD results can be compared and evaluated with our mixed structure of pseudo α-helix and β-turn from our experimental results.

Discussion

NMR signal assignments of P99 peptide were made by using homonuclear proton correlation 2D NMR experiments including COSY, TOCSY and NOESY. Dipolar connectivities from amide protons to α- and amide protons were used for sequential signal assignments. NMR based solution structures were determined with important NOEs and 2D-NOE back calculation method. Out of P99 residues (KGTYG LSCQR DPNTG RLNGE) Gln[9] to Thr[13] clearly demonstrate a β-turn conformation as shown in Figure 5. As a result of NMR based solution state structure determination of Apo B-100 partial peptides P99.

The final result of peptide structure determination is presented as a best position of a group of conformers for pairwise minimum root mean square deviation (RMSD) relative to a predetermined conformer. CD spectra show that P99 has mixed structure of α-helix and β-turn. It was found that peptides have a characteristic β-turn structure possibly derived from the proline in the middle of sequences as compared. It is believed that lysine residue may play important role in the recognition of the monoclonal antibodies in via peroxidation with MDA.

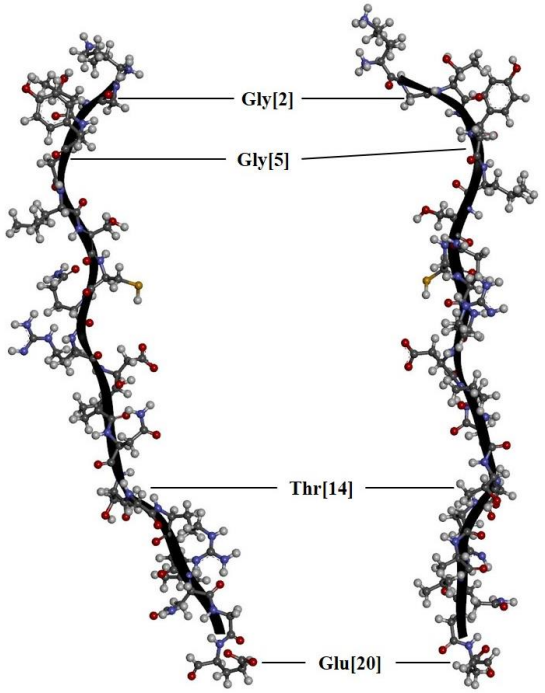

Figure 5. Stereo-views of P99 showing best-fit super positions of all atoms (excluding protons).

Further molecular docking studies with current results may provide the antigen specificity and regulation of surface conformational changes in the mechanism of apo lipoproteins playing an important role in lipid transport and metabolic process in blood stream.

Acknowledgements

This work was supported by the research fund of Hanyang University (HY-2020-G).

References

1. R. W. Mahley, T. L. Innerarity, S. C. Jr. Rall and K. H. Wesgraber, *J. Lipid Res.* **25**, 1277 (1984)

2. R. A. Davis, *Biochem. Lipid* (1991)
3. B. H. Browman, *Hepatic Plasma Proteins Mechanisms of Function and Regulations,* Academic Press, Inc., London (1993)
4. V. N. Schumaker, M. L. Phillips and J. E. Chatterton, *Adv. Protein* **45**, 205 (1994)
5. S. H. Chen, C. Y. Yang, P. F. Chen, D. Setzer, M. Tamimura, W. H. Li, A. M. Gotto and L. J. Chan, *Biol. Chem.* **261**, 12918 (1986)
6. T. J.Knott, R. J.Pease, L. M.Powell, S. C.Wallis, S. C.Rall Jr, T. L. Innerarity, B. Blackhart, W. H. Taylor, Y. Marcel, R. Milne, D. Johnson, M. Fuller, A. J. Lusis, B. J. McCarthy, R. W. Mahley, B. L. Wilson and J. Scott, *Nature* **323**, 734 (1986)
7. M. L. Phillips and V. N. Schumaker, *J. Lipid Res.* **30**, 415 (1989)
8. A. D. Cardin and R. L. Jackson, *Biochem. Biophys. Acta.* **877**, 366 (1986)
9. G. C. Chen, S. Zhu, D. A. Hardman, J. W. Schilling, K. Lau and J. P. Kane, *J. Biol. Chem*. **264**, 14369 (1989)
10. R. A. Davis, R. N. Thrift, C. C. Wu and K. E. Howell, *J. Biol. Chem.* **265**, 10005 (1990)
11. C. Ettelaie, P. I. Haris, N. J. James, B. Wilbourn, J. M. Adam and K. R. Bruckdorfer, *Biochem. Biophy. Acta*. **1345**, 237 (1997)
12. C. Y. Yang, S. H. Chen, S. H. Gianturco, W. A. Bradley, J. T. Sparrow, M. Tanimura, W. H. Li, D. A. Sparrow, S. Deloof, M. Rosseneu, F. S. Lee, Z. W. Gu, A. M. Gotto and L. Chan, *Nature* **323**, 738 (1986)
13. H. Jamila, C. H. Chua, J. K. Dickson, Y. Chenb, M. Yana, S. A. Billerb, R. C. Gregga, J. R. Wetteraua and D. A. Gordana, *J. Lipid Res.* **39**, 1448 (1998)
14. S. W. Law, S. M. Grant and K. Hlguchi, *Proc. Nati. Acad. Sci. U. S. A.* **83**, 8142 (1988)
15. U. Stelnbrecher, *J. Biol. Chem.* **262**, 3603 (1987)
16. S. Lee, D. Kim, H. Kim, Y. Lee and H. Won, *Bull. Korean Chem. Soc*. **25**, 12 (2004)
17. D. Kim, J. Rho and H. Won, *J. Kor. Magn. Reson. Soc*. **3**, 44 (1999)
18. N. J. Greenfield, *Trac-Trends Anal. Chem*. **18**, 236 (1999)
19. G. Kim and H. Won, *J. Kor. Magn. Reson. Soc*. **20**, 96 (2016)